Available online at www.sciencedirect.com
ScienceDirect
Journal of Sound and Vibration 306 (2007) 636–656
JOURNAL OF SOUND AND VIBRATION
www.elsevier.com/locate/jsvi

Wave propagation, reflection and transmission in curved beams

S.-K. Lee, B.R. Mace*, M.J. Brennan

Institute of Sound and Vibration Research, University of Southampton, Highfield, Southampton SO17 1BJ, UK

Received 2 February 2007; received in revised form 30 May 2007; accepted 2 June 2007

Abstract

Wave motion in thin, uniform, curved beams with constant curvature is considered. The beams are assumed to undergo only in-plane motion, which is described by the sixth-order coupled differential equations based on Flügge's theory. In the wave domain the motion is associated with three independent wave modes. A systematic wave approach based on reflection, transmission and propagation of waves is presented for the analysis of structures containing curved beam elements. Displacement, internal force and propagation matrices are derived. These enable transformations to be made between the physical and wave domains and provide the foundation for systematic application of the wave approach to the analysis of waveguide structures with curved beam elements. The energy flow associated with waves in the curved beam is also discussed. It is seen that energy can be transported independently by the propagating waves and also by the interaction of a pair of positive and negative going wave components which are non-propagating, i.e. their wavenumbers are imaginary or complex. A further transformation can be made to power waves, which can transport energy independently. Numerical examples are given to illustrate the wave approach. The first concerns power transmission and reflection through a U-shaped connector between two straight beams while the second concerns the free vibration of finite curved beams where results are compared to other published results.

1. Introduction

Curved beams are used widely in built-up structures and hence their dynamic behaviour is of interest. Previous work in this area has been summarised in several articles, for example [1–3]. Wu and Lundberg [4] have investigated the transmission of energy through a curved section connecting two straight beams. They presented numerical results in the form of polar radiation diagrams for beams with different curvatures. Walsh and White [5] considered the energy flow associated with a single propagating wave component in a curved beam based on four different theories—Love's theory, Flügge's theory and the corrections for rotary inertia and shear deformation. They derived expressions which relate the power to the extensional, bending and shear waves. Kang et al. [6] applied the wave approach based on the reflection, transmission and propagation of waves to obtain the natural frequencies of finite curved beams.

The main aim of this paper is to describe a systematic wave approach based on reflection, transmission and propagation of waves and to use this to determine the energy flow characteristics of waves in a thin, curved

*Corresponding author. Tel.: +44 23 8059 2311; fax: +44 23 8059 3190.
E-mail address: brm@isvr.soton.ac.uk (B.R. Mace).

0022-460X/$ - see front matter © 2007 Elsevier Ltd. All rights reserved.
doi:10.1016/j.jsv.2007.06.001

Nomenclature

List of symbols

a, d	amplitudes of waves
a, **b**, **d**	vector of amplitudes of waves
A	cross-sectional area
b	width
c_l	phase velocity of longitudinal wave
C	arbitrary constant
$\mathrm{d}s$	arc length
$\mathrm{d}\theta$	arc angle
E	modulus of elasticity
E	unitary matrix, the columns of which are eigenvectors of **P**
f	vector of generalised internal forces
F	propagation matrix
h	thickness
I	the second moment of area
I	identity matrix
k	wavenumber
k_b	bending wavenumber
k_l	longitudinal wavenumber
L	length
M	bending moment
N	normal force
p	vector of amplitudes of power waves
P	power matrix, Hermitian
Q	shear force
R	radius of curvature
R	reflection matrix
s	circumferential coordinate
t	time
T	transmission matrix
u	tangential displacement of the centreline
V	diagonal matrix consisting of the (real) eigenvalues of **P**
w	radial displacement of the centreline
w	vector of generalised displacements
z	coordinate along the normal to the centreline
α	ratio of tangential displacement to radial displacement
κ	curvature, $\kappa = 1/R$
λ	wavelength
ξ	dimensionless wavenumber
Π	power
ρ	density
ϱ	power reflection coefficient
τ	power transmission coefficient
φ	rotation of the normal to the centreline
$\boldsymbol{\phi}$	column vector of $\boldsymbol{\Phi}$
$\boldsymbol{\Phi}$	internal force matrix
χ	dimensionless radius of gyration
$\boldsymbol{\psi}$	column vector of $\boldsymbol{\Psi}$
$\boldsymbol{\Psi}$	displacement matrix
ω	angular frequency
ω_c	ring frequency
Ω	dimensionless angular frequency

Subscripts

B	denote bending motion
L	denote longitudinal motion
N	denote nearfield wave

Superscripts

$+$	denote positive-going direction in x-axis
$-$	denote negative-going direction in x-axis
$\cap$	combined with **R** and **T**, denote the case where waves are incident from the right-hand side

Operators

T	transpose
H	Hermitian
*	complex conjugate
$\mathrm{Re}(\cdot)$	real part of a quantity

beam. The approach is also valid when rotary inertia, shear deformations and damping are important, but these effects are neglected here. Attention is focused on in-plane motion and Flügge's theory is used. The motion is described in terms of six independent (or uncoupled) wave components. Examples are given to show how the approach can be used for the analysis of structures with curved elements.

In Section 2, the dispersion relation and the ratio of tangential displacement to radial displacement for the six wave components are obtained. In Section 3 displacement, internal force and propagation matrices are derived. These enable transformations to be made between the physical and wave domains and provide the foundation for systematic application of the wave approach [7] to waveguide structures with curved elements.

In Section 4, the energy flow associated with the wave components is obtained in a systematic way. Their contributions are classified according to different conditions for the wavenumbers. The energy flow paths are identified at a frequency given. Energy can be transported independently by propagating waves or by pairs of wave components with imaginary or complex wavenumbers. A further transformation is found to power wave components—these propagate energy independently through the curved beam. In Section 5 numerical examples are considered. The first concerns power transmission and reflection through a U-shaped connector between two straight beams while the second concerns the free vibration of finite curved beams where results derived here are compared to results published in the literature.

2. In-plane wave motion in curved beams

Consider a small segment of a curved beam with a subtended angle $d\theta$ at the centre of curvature as shown in Fig. 1 (a list of symbols is given in the Nomenclature). The centreline is the locus of the centroids of each cross-sectional segment. The circumferential coordinate along the centreline is denoted by s and the radial coordinate normal to the centreline is z. The displacements of the centreline in the radial and tangential directions are denoted by w and u, respectively. The arc length of the segment is $ds = R\,d\theta$, where R is radius of curvature of the centreline.

Neglecting the effects of shear deformation and rotary inertia, the governing equations for free vibration in the radial and tangential directions are given by [5]

$$-EI\left(\frac{\partial^4 w}{\partial s^4}+\frac{2}{R^2}\frac{\partial^2 w}{\partial s^2}+\frac{w}{R^4}\right)-\frac{EA}{R}\left(\frac{w}{R}+\frac{\partial u}{\partial s}\right)=\rho A\frac{\partial^2 w}{\partial t^2},\quad EA\left(\frac{\partial^2 u}{\partial s^2}+\frac{1}{R}\frac{\partial w}{\partial s}\right)=\rho A\frac{\partial^2 u}{\partial t^2}, \tag{1a,b}$$

where E is the Young's modulus, I the second moment of area, A the cross-sectional area, ρ the density and t is time. The rotation φ of the cross-section and the normal force N, bending moment M, and shear force Q are given by [5]

$$\varphi=-\frac{u}{R}+\frac{\partial w}{\partial s},\quad N=EA\left(\frac{w}{R}+\frac{\partial u}{\partial s}\right)+\frac{EI}{R}\left(\frac{w}{R^2}+\frac{\partial^2 w}{\partial s^2}\right),\quad M=EI\left(\frac{w}{R^2}+\frac{\partial^2 w}{\partial s^2}\right),$$
$$Q=-EI\left(\frac{1}{R^2}\frac{\partial w}{\partial s}+\frac{\partial^3 w}{\partial s^3}\right). \tag{2a, b, c, d}$$

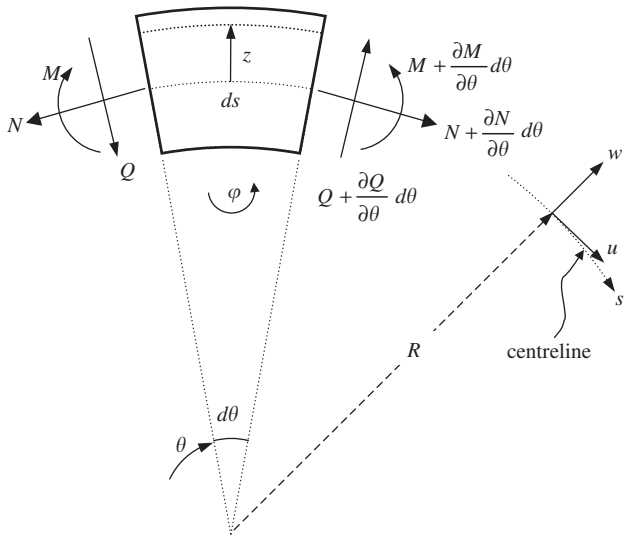

Fig. 1. Differential element of a thin, curved beam and sign convention of physical quantities.

Eqs. (1) and (2) describe the in-plane motion of thin, uniform, curved beams with constant curvature based on Flügge's theory. When R tends to infinity, the radial and tangential displacements decouple and the equations become those for a uniform, straight beam.

2.1. Dispersion relationships

Using Eqs. (1) and (2), a transformation from the physical domain into the wave domain can be made and the dispersion relationship for each wave component is obtained. The radial and tangential displacements satisfying Eq. (1) are assumed to be time harmonic and of the form:

$$w(s,t) = C_w e^{i(\omega t - ks)}, \quad u(s,t) = C_u e^{i(\omega t - ks)}, \tag{3a,b}$$

where C_w and C_u are constants and k is the wavenumber for the curved beam. Substituting Eq. (3a,b) into Eq. (1) gives

$$\begin{bmatrix} \frac{I}{AR^2}(k^2R^2-1)^2 + 1 - \frac{\rho}{E}R^2\omega^2 & -ikR \\ ikR & k^2R^2 - \frac{\rho}{E}R^2\omega^2 \end{bmatrix} \begin{Bmatrix} C_w \\ C_u \end{Bmatrix} = 0. \tag{4}$$

Setting the determinant of the matrix in Eq. (4) to zero gives the dispersion equation

$$k^6 - (k_L^2 + 2\kappa^2)k^4 + (\kappa^4 - k_B^4 + 2\kappa^2 k_L^2)k^2 - (\kappa^4 k_L^2 + \kappa^2 k_B^4 - k_L^2 k_B^4) = 0, \tag{5}$$

where $k_L = \sqrt{\rho\omega^2/E}$ and $k_B = \sqrt[4]{\rho A\omega^2/EI}$ are the longitudinal and bending wavenumbers for a straight beam, respectively, and $\kappa = 1/R$ is the curvature. The beam is undamped so that k_L and k_B are real.

Since Eq. (5) is a cubic equation in k^2, there are three pairs of solutions at any given frequency, three for positive-going waves and three for negative-going waves. When κ tends to zero, four wavenumbers asymptote to the bending wavenumbers and two wavenumbers asymptote to the longitudinal wavenumbers. The ring frequency, ω_c, which is the non-zero frequency corresponding to $k = 0$, is given by

$$\omega_c = \frac{c_L}{R}\sqrt{1 + \frac{I}{AR^2}}, \tag{6}$$

where c_L is the longitudinal phase velocity for a uniform straight bar. Note that this cut-off frequency obtained from Flügge's theory slightly differs from that obtained from Love's theory by the term I/AR^2. This difference is likely to be negligible since I/AR^2 (or h/R for a rectangular beam) should be small for the thin beam assumption to be valid.

Solutions to Eq. (5) are obtained as described in Appendix A. The non-dimensional radius of gyration, wavenumber and frequency are introduced and are, respectively, given by

$$\chi = \sqrt{\frac{I}{AR^2}}, \quad \xi = kR, \quad \Omega = \frac{\omega R}{c_L} \tag{7a,b,c}$$

so that Eq. (5) can be re-written as

$$\{\chi^2(\xi^2-1)^2 + 1 - \Omega^2\}(\xi^2 - \Omega^2) - \xi^2 = 0. \tag{8}$$

Fig. 2 shows the wavenumbers for the curved beam with $\chi^2 = 1/1200$, which corresponds to $h/R = 0.1$ if the beam is rectangular. The frequency range considered is far below the "cross-over" frequency, which is the frequency when the wavenumber for the predominantly flexural wave is equal to the wavenumber for the predominantly longitudinal wave, given by $\Omega = 1/\chi \approx 34.6$. At this frequency the longitudinal wavelength $\lambda_L = 2\pi\chi$ [5]. The behaviour falls into four frequency regions and is characteristic of curved beams of other dimensions. There are five bifurcation points at which there are qualitative changes in the wavenumbers. The lowest two bifurcations are located near the frequency $\Omega_1 \approx \chi/3 \approx 10^{-2}$. At this frequency four propagating waves (with real wavenumbers) change into two decaying oscillating waves whose wavenumbers are complex conjugates. The next two bifurcations are located near the frequency $\Omega_2 \approx 4\chi \approx 0.16$ where the bending wavelength $\lambda_B = \pi R$. Here the two decaying oscillating waves change into four evanescent waves which have

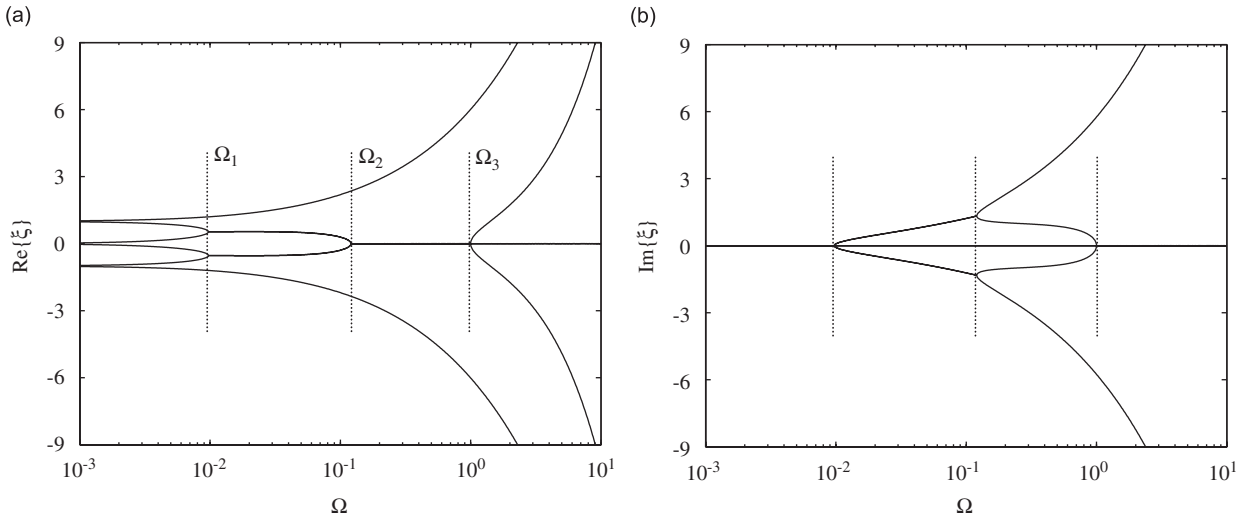

Fig. 2. Dispersion relations for wave modes in the curved beam with $\chi^2 = 1/1200$: (a) real values of ξ and (b) imaginary values of ξ.

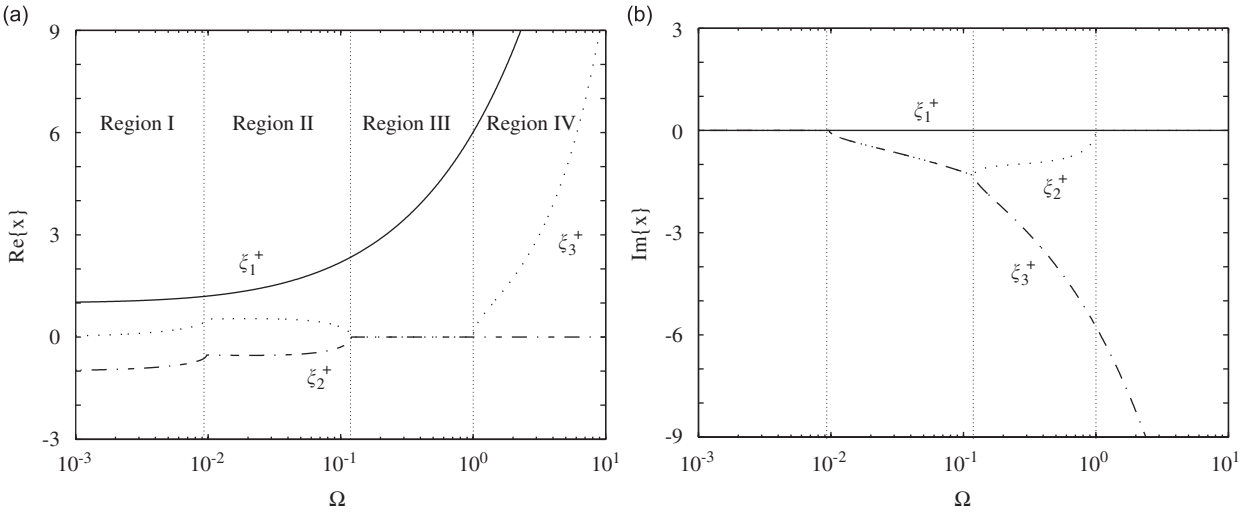

Fig. 3. Dispersion relations for positive-going waves in the curved beam with $\chi^2 = 1/1200$: (a) real values of ξ and (b) imaginary values of ξ.

purely imaginary wavenumbers. The highest bifurcation point is at the ring frequency $\Omega_3 = 1$, i.e. when $\lambda_L = 2\pi R$. Here two of the evanescent waves change into two propagating waves.

The wavenumbers of positive-going waves are defined to be such that

$$\mathrm{Im}\{k\} \leqslant 0, \quad \mathrm{Re}\{\partial k/\partial \omega\} > 0 \text{ if } \mathrm{Im}\{k\} = 0. \tag{9a,b}$$

Eq. (9a) indicates that, if the imaginary value of the wavenumber of a positive-going wave is non-zero, the amplitude of the wave decays in the positive s direction. If the imaginary value is zero, Eq. (9b) indicates that the energy transport velocity associated with a positive-going wave should be positive.

Fig. 3 shows the wavenumbers for the positive-going waves in the curved beam with $\chi^2 = 1/1200$. In the figure the frequency range is divided into four regions by the bifurcation points. In region I, the wavenumbers for the three modes are all purely real so that all the wave modes propagate along the curved beam. One interesting feature is that the (real) wavenumbers for the second mode ξ_2^+ are negative in this region. Thus the

phase velocity of the wave mode is negative while the energy is transported in the positive s direction, i.e. a wave transports energy in the direction opposite to the direction of the phase velocity. Such behaviour—the phase and group velocities having opposite signs—is commonly observed in waveguides other than those of the simplest types. In region II, ξ_2^+ is complex and, since $\xi_2^+ = -(\xi_3^+)^*$, this represents a spatially decaying standing wave as discussed above. Only the first mode can propagate. In region III, also, only the first mode propagates. The other wave modes are both evanescent, i.e., they decay without a change in phase. In region IV, ξ_3^+ becomes purely real, representing a propagating wave. In this region the wavenumbers are broadly analogous to those of bending (ξ_1^+, ξ_2^+) and extensional waves (ξ_3^+) in a straight beam.

2.2. Displacement ratio

The radial and tangential displacements of the curved beam are not independent of each other. From Eq. (4), the ratio $\alpha = C_u/C_w$ of these displacements is given by

$$\alpha = \frac{\mathrm{i}\kappa k}{k_L^2 - k^2}. \tag{10}$$

The six waves associated with the motion of the curved beam are now specified by subscript i, where $i = 1, 2, \ldots, 6$, where $i = 1, 2, 3$ denote the three positive-going waves, respectively, and $i = 4, 5, 6$ denote the corresponding negative-going waves. The ratio α_i for a wave i is given by replacing k with k_i in Eq. (10) to give

$$\alpha_i = \frac{\mathrm{i}\kappa k_i}{k_L^2 - k_i^2}, \quad i = 1, 2, \ldots, 6. \tag{11}$$

Note that $\alpha_{4,5,6} = -\alpha_{1,2,3}$ since $k_{4,5,6} = -k_{1,2,3}$.

Fig. 4 shows the displacement ratio for the three positive-going waves for the curved beam with $\chi^2 = 1/1200$. The four regions shown in Fig. 3 are not marked for clarity, but can be inferred from the discontinuous behaviour of the curves. It can be seen that the radial motion is dominant for the first wave mode since $|\alpha_1| < 1$ in the frequency range considered. In region II $|\alpha_2| = |\alpha_3|$. In regions III and IV, the radial motion is dominant for the second mode. Near the ring frequency $\Omega = 1$, the radial motion is dominant for the third mode (the magnitude of α_3 is zero at the ring frequency) but, as frequency increases, the tangential motion becomes dominant. The phase difference between the displacement components is between $\pi/2$ and $-\pi/2$ radians.

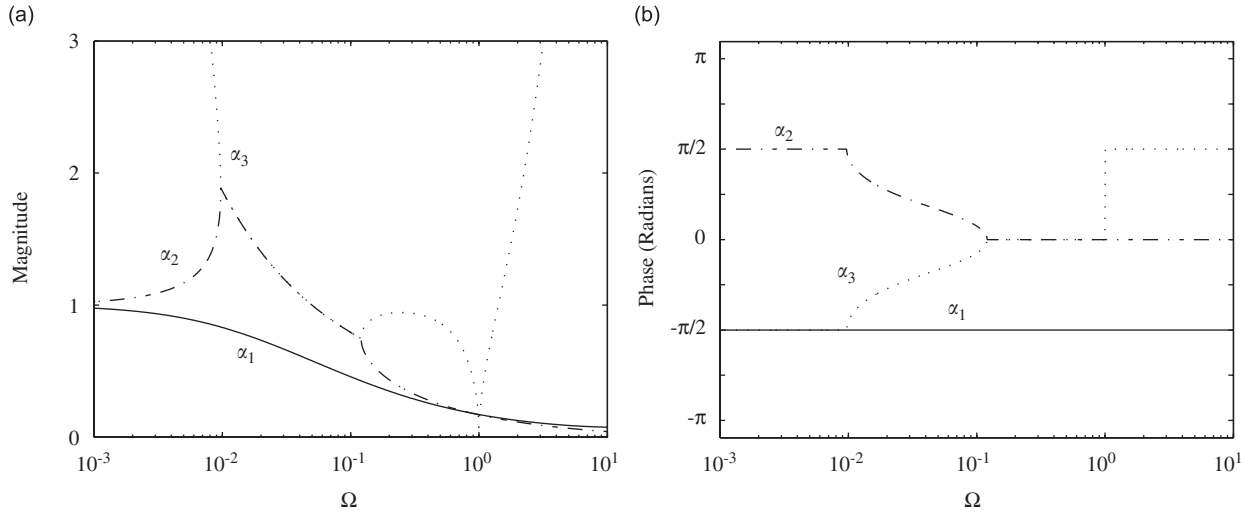

Fig. 4. Ratio of the tangential displacement to the radial displacement, $\alpha = C_u/C_w$, for the curved beam with $\chi^2 = 1/1200$: (a) magnitude of α and (b) phase of α.

3. Matrix representation of wave motion

A systematic methodology for wave analysis based on reflection, transmission and propagation of waves is provided by the definition of displacement, internal force and propagation matrices [7]. In this section, the matrices for the curved beam are presented. Since the curved beam is a three-mode system, the relevant vectors and matrices are of order 3×1 and 3×3, respectively.

Assuming the displacements to be of the form given by Eq. (3), the radial and tangential displacements of the beam are given, respectively, by

$$w(s) = C_1 e^{-ik_1 s} + C_2 e^{-ik_2 s} + C_3 e^{-ik_3 s} + C_4 e^{-ik_4 s} + C_5 e^{-ik_5 s} + C_6 e^{-ik_6 s},$$
$$u(s) = \alpha_1 C_1 e^{-ik_1 s} + \alpha_2 C_2 e^{-ik_2 s} + \alpha_3 C_3 e^{-ik_3 s} + \alpha_4 C_4 e^{-ik_4 s} + \alpha_5 C_5 e^{-ik_5 s} + \alpha_6 C_6 e^{-ik_6 s}. \quad (12a, b)$$

Eq. (12a,b) are not in a suitable form for later development since, at high frequencies (where the radial and tangential displacements decouple), α_3 and α_6 tend to infinity. Instead, the radial and tangential displacements are expressed as

$$w(s) = C_1 e^{-ik_1 s} + C_2 e^{-ik_2 s} + (\alpha_3)^{-1} C_3 e^{-ik_3 s} + C_4 e^{-ik_4 s} + C_5 e^{-ik_5 s} + (\alpha_6)^{-1} C_6 e^{-ik_6 s},$$
$$u(s) = \alpha_1 C_1 e^{-ik_1 s} + \alpha_2 C_2 e^{-ik_2 s} + C_3 e^{-ik_3 s} + \alpha_4 C_4 e^{-ik_4 s} + \alpha_5 C_5 e^{-ik_5 s} + C_6 e^{-ik_6 s}. \quad (13a, b)$$

Now, at high frequencies, all the coefficients $\alpha_{1,2,4,5}$ and $(\alpha_{3,6})^{-1}$ tend to zero.

The generalised displacements and corresponding internal forces can be grouped in the vectors

$$\mathbf{w} = \begin{Bmatrix} w \\ \varphi \\ u \end{Bmatrix}, \quad \mathbf{f} = \begin{Bmatrix} Q \\ M \\ N \end{Bmatrix}. \quad (14a,b)$$

Note that the rotation φ and internal forces Q, M and N are obtained from Eqs. (2) and (13). The wave vectors consisting of the amplitudes of the waves are defined by

$$\mathbf{a}^+(s) = \begin{Bmatrix} C_1 e^{-ik_1 s} \\ C_2 e^{-ik_2 s} \\ C_3 e^{-ik_3 s} \end{Bmatrix}, \quad \mathbf{a}^-(s) = \begin{Bmatrix} C_4 e^{-ik_4 s} \\ C_5 e^{-ik_5 s} \\ C_6 e^{-ik_6 s} \end{Bmatrix}. \quad (15a,b)$$

The displacement and internal force vectors are related to the vectors of wave amplitudes by [7]

$$\mathbf{w} = \mathbf{\Psi}^+ \mathbf{a}^+ + \mathbf{\Psi}^- \mathbf{a}^-, \quad \mathbf{f} = \mathbf{\Phi}^+ \mathbf{a}^+ + \mathbf{\Phi}^- \mathbf{a}^-, \quad (16)$$

where the matrices $\mathbf{\Psi}$ and $\mathbf{\Phi}$ define the transformation from the wave domain to the physical domain. They are given by

$$\mathbf{\Psi}^+ = [\boldsymbol{\psi}_1 \quad \boldsymbol{\psi}_2 \quad \boldsymbol{\psi}_3], \quad \mathbf{\Psi}^- = [\boldsymbol{\psi}_4 \quad \boldsymbol{\psi}_5 \quad \boldsymbol{\psi}_6], \quad \mathbf{\Phi}^+ = \begin{bmatrix} \boldsymbol{\phi}_1 & \boldsymbol{\phi}_2 & \boldsymbol{\phi}_3 \end{bmatrix}, \quad \mathbf{\Phi}^- = \begin{bmatrix} \boldsymbol{\phi}_4 & \boldsymbol{\phi}_5 & \boldsymbol{\phi}_6 \end{bmatrix}, \quad (17a,b,c,d)$$

where the column vectors $\boldsymbol{\psi}_i$ and $\boldsymbol{\phi}_i$ for $i = 1, 2, 4, 5$ are

$$\boldsymbol{\psi}_i = \begin{Bmatrix} 1 \\ -(\kappa\alpha_i + ik_i) \\ \alpha_i \end{Bmatrix}, \quad \boldsymbol{\phi}_i = \begin{Bmatrix} iEIk_i(\kappa^2 - k_i^2) \\ EI(\kappa^2 - k_i^2) \\ EA(\kappa - ik_i\alpha_i) + EI\kappa(\kappa^2 - k_i^2) \end{Bmatrix} \quad (18a,b)$$

and $\boldsymbol{\psi}_i$ and $\boldsymbol{\phi}_i$ for $i = 3, 6$ are

$$\boldsymbol{\psi}_i = \frac{1}{\alpha_i} \begin{Bmatrix} 1 \\ -(\kappa\alpha_i + ik_i) \\ \alpha_i \end{Bmatrix}, \quad \boldsymbol{\phi}_i = \frac{1}{\alpha_i} \begin{Bmatrix} iEIk_i(\kappa^2 - k_i^2) \\ EI(\kappa^2 - k_i^2) \\ EA(\kappa - ik_i\alpha_i) + EI\kappa(\kappa^2 - k_i^2) \end{Bmatrix}. \quad (19a,b)$$

If $\Omega \gg 1$, when the radial and tangential displacements decouple, the matrices $\mathbf{\Psi}^+$ and $\mathbf{\Phi}^+$ asymptote to

$$\mathbf{\Psi}^+ \approx \begin{bmatrix} 1 & 1 & 0 \\ -\mathrm{i}k_B & -k_B & 0 \\ 0 & 0 & 1 \end{bmatrix}, \quad \mathbf{\Phi}^+ \approx \begin{bmatrix} -\mathrm{i}EIk_B^3 & EIk_B^3 & 0 \\ -EIk_B^2 & EIk_B^2 & 0 \\ 0 & 0 & -\mathrm{i}EAk_L \end{bmatrix}, \tag{20a,b}$$

i.e., the matrices are composed of those of the uniform straight beam and the other elements are zero, as expected. Using these matrices, the reflection and transmission matrices for arbitrary discontinuities or for boundaries can be found in a simple manner (e.g. Ref. [7], or see Section 5 for an example).

The propagation matrix $\mathbf{F}$, describing propagation of waves over a distance L along the curved beam, is given by

$$\mathbf{F}(L) = \begin{bmatrix} \mathrm{e}^{-\mathrm{i}k_1 L} & 0 & 0 \\ 0 & \mathrm{e}^{-\mathrm{i}k_2 L} & 0 \\ 0 & 0 & \mathrm{e}^{-\mathrm{i}k_3 L} \end{bmatrix}. \tag{21}$$

Note that the propagation matrix is diagonal (i.e. the waves are not coupled during propagation) and the diagonal elements are independent of position.

4. Energy flow in curved beams

The time-averaged power Π associated with waves in one-dimensional structures can be expressed as [7]

$$\Pi = \tfrac{1}{2}\mathbf{a}^{\mathrm{H}}\mathbf{P}\mathbf{a}, \tag{22}$$

where $\mathbf{a} = [\,(\mathbf{a}^+)^{\mathrm{T}} \quad (\mathbf{a}^-)^{\mathrm{T}}\,]^{\mathrm{T}}$ and the power matrix $\mathbf{P}$ is given by

$$\mathbf{P} = \frac{\mathrm{i}\omega}{2}\left[\begin{bmatrix} (\mathbf{\Psi}^+)^{\mathrm{H}}\mathbf{\Phi}^+ & (\mathbf{\Psi}^+)^{\mathrm{H}}\mathbf{\Phi}^- \\ (\mathbf{\Psi}^-)^{\mathrm{H}}\mathbf{\Phi}^+ & (\mathbf{\Psi}^-)^{\mathrm{H}}\mathbf{\Phi}^- \end{bmatrix} - \begin{bmatrix} (\mathbf{\Phi}^+)^{\mathrm{H}}\mathbf{\Psi}^+ & (\mathbf{\Phi}^+)^{\mathrm{H}}\mathbf{\Psi}^- \\ (\mathbf{\Phi}^-)^{\mathrm{H}}\mathbf{\Psi}^+ & (\mathbf{\Phi}^-)^{\mathrm{H}}\mathbf{\Psi}^- \end{bmatrix}\right]. \tag{23}$$

Since the matrix $\mathbf{P}$ is Hermitian, the power Π is always real.

Substituting Eq. (17) into Eq. (23) gives the power matrix $\mathbf{P}$ for the curved beam. Then P_{mn}, the (m,n)th element of the matrix, for $m = 1,\ldots,6$ and $n = 1,\ldots,6$ is

$$P_{mn} = \frac{\mathrm{i}\omega}{2}(\boldsymbol{\psi}_m^{\mathrm{H}}\boldsymbol{\phi}_n - \boldsymbol{\phi}_m^{\mathrm{H}}\boldsymbol{\psi}_n). \tag{24}$$

4.1. Energy flow associated with wave components

In Appendix B, P_{mn} is given for all possible pairs of the six wave components. It is seen that energy can be transported in three cases:

- by a single wave with real wavenumber (i.e., a propagating wave);
- by interaction between two opposite-going waves of one mode, for which the wavenumber is purely imaginary (i.e., two opposite-going nearfield waves);
- by interaction between two opposite-going waves from different modes, for which the wavenumbers are a complex conjugate pair.

These results are consistent with the work by Langley [8] for a general one-dimensional dynamic system.

4.2. Energy flow at a single frequency

In this section, the energy flow mechanisms (carriers) at a given frequency are summarised using results from Appendix B.

(i) *In region I*: All waves are propagating and the wavenumbers are real in this frequency range. The power matrix becomes diagonal and is given by

$$\mathbf{P} = \begin{bmatrix} P_{11} & 0 & 0 & 0 & 0 & 0 \\ 0 & P_{22} & 0 & 0 & 0 & 0 \\ 0 & 0 & P_{33} & 0 & 0 & 0 \\ 0 & 0 & 0 & -P_{11} & 0 & 0 \\ 0 & 0 & 0 & 0 & -P_{22} & 0 \\ 0 & 0 & 0 & 0 & 0 & -P_{33} \end{bmatrix}, \tag{25}$$

where the diagonal elements are

$$P_{11} = \omega EIk_1 \left\{ 2(k_1^2 - \kappa^2) + \frac{k_B^4 \kappa^2}{(k_L^2 - k_1^2)^2} \right\},$$

$$P_{22} = \omega EIk_2 \left\{ 2(k_2^2 - \kappa^2) + \frac{k_B^4 \kappa^2}{(k_L^2 - k_2^2)^2} \right\},$$

$$P_{33} = \omega EA \frac{k_L^2}{k_3} \left\{ 1 + \frac{2(k_3^2 - \kappa^2)(k_L^2 - k_3^2)^2}{k_B^4 \kappa^2} \right\}. \tag{26a, b, c}$$

The power associated with the vector of wave amplitudes $\mathbf{a}$ is given by Eq. (22). For example, suppose $\mathbf{a} = \begin{bmatrix} a_1 & 0 & 0 & 0 & 0 & 0 \end{bmatrix}^{\mathrm{T}}$, i.e. there is only a positive-going wave of the first mode of amplitude a_1. Then the power associated with the wave is given by

$$\Pi = \frac{1}{2} \sum_j P_{jj} |a_j|^2 = \frac{1}{2} P_{11} |a_1|^2. \tag{27}$$

(ii) *In region II*: The non-zero elements are P_{11}, P_{26}, P_{35} and their counterparts P_{44}, P_{62} and P_{53}. In this case $P_{26} = P_{62}^* = P_{35}^* = P_{53}$. Thus the power matrix is given by

$$\mathbf{P} = \begin{bmatrix} P_{11} & 0 & 0 & 0 & 0 & 0 \\ 0 & 0 & 0 & 0 & 0 & P_{26} \\ 0 & 0 & 0 & 0 & P_{26}^* & 0 \\ 0 & 0 & 0 & -P_{11} & 0 & 0 \\ 0 & 0 & P_{26} & 0 & 0 & 0 \\ 0 & P_{26}^* & 0 & 0 & 0 & 0 \end{bmatrix}, \tag{28}$$

where

$$P_{26} = -\frac{\mathrm{i}\omega EI}{\kappa} \left(k_2^2 - (k_2^*)^2\right) \left((k_2^*)^2 - k_1^2\right). \tag{29}$$

For example, suppose $\mathbf{a} = [\,0 \quad a_2 \quad 0 \quad 0 \quad 0 \quad a_6\,]^{\mathrm{T}}$. Then the power is given by

$$\Pi = \mathrm{Re}\,(P_{26}(a_2)^* a_6), \tag{30}$$

where $\mathrm{Re}\,(\cdot)$ denotes the real part of the quantity. The direction of energy flow depends on the phases of P_{26}, $(a_2)^*$ and a_6.

The power matrix is not diagonal in this region. A further transformation can be defined using a power basis, where energy is transported independently by a single component, using the eigenvalues and eigenvectors of the power matrix. Let $\mathbf{V}$ be the diagonal matrix consisting of the (real) eigenvalues and $\mathbf{E}$ be the (unitary) matrix whose columns are the eigenvectors of $\mathbf{P}$. Since $\mathbf{P} = \mathbf{E}\mathbf{V}\mathbf{E}^{-1}$, Eq. (22) can be written as

$$\Pi = \tfrac{1}{2} \mathbf{p}^{\mathrm{H}} \mathbf{V} \mathbf{p}, \tag{31}$$

where $\mathbf{p} = \mathbf{E}^{-1}\mathbf{a}$ is a vector of power wave amplitudes. Since $\mathbf{V}$ is diagonal, Eq. (31) indicates that energy is transported independently by the individual power wave components of $\mathbf{p}$. In this region $\mathbf{V}$ and $\mathbf{E}$ are given by

$$\mathbf{V} = \begin{bmatrix} P_{11} & 0 & 0 & 0 & 0 & 0 \\ 0 & |P_{26}| & 0 & 0 & 0 & 0 \\ 0 & 0 & |P_{26}| & 0 & 0 & 0 \\ 0 & 0 & 0 & -P_{11} & 0 & 0 \\ 0 & 0 & 0 & 0 & -|P_{26}| & 0 \\ 0 & 0 & 0 & 0 & 0 & -|P_{26}| \end{bmatrix},$$

$$\mathbf{E} = \begin{bmatrix} 1 & 0 & 0 & 0 & 0 & 0 \\ 0 & \frac{1}{\sqrt{2}} & 0 & 0 & 0 & \frac{\phi}{\sqrt{2}} \\ 0 & 0 & \frac{1}{\sqrt{2}} & 0 & \frac{\phi^*}{\sqrt{2}} & 0 \\ 0 & 0 & 0 & 1 & 0 & 0 \\ 0 & 0 & \frac{\phi}{\sqrt{2}} & 0 & -\frac{1}{\sqrt{2}} & 0 \\ 0 & \frac{\phi^*}{\sqrt{2}} & 0 & 0 & 0 & -\frac{1}{\sqrt{2}} \end{bmatrix}, \tag{32a, b}$$

where $\phi = P_{26}/|P_{26}|$.

(iii) *In region III*: The power matrix is given by

$$\mathbf{P} = \begin{bmatrix} P_{11} & 0 & 0 & 0 & 0 & 0 \\ 0 & 0 & 0 & 0 & P_{25} & 0 \\ 0 & 0 & 0 & 0 & 0 & P_{36} \\ 0 & 0 & 0 & -P_{11} & 0 & 0 \\ 0 & P_{25}^* & 0 & 0 & 0 & 0 \\ 0 & 0 & P_{36}^* & 0 & 0 & 0 \end{bmatrix}, \tag{33}$$

where the element P_{11} is the same as Eq. (26a) and

$$P_{25} = -\omega E I k_2 \left\{ 2(k_2^2 - \kappa^2) + \frac{k_B^4 \kappa^2}{(k_l^2 - k_2^2)^2} \right\}, \quad P_{36} = -\omega E A \frac{k_L^2}{k_3} \left\{ 1 + \frac{2(k_3^2 - \kappa^2)(k_L^2 - k_3^2)^2}{k_B^4 \kappa^2} \right\}. \tag{34a,b}$$

The elements P_{25} and P_{36} are negative-imaginary in this region so that $\mathbf{V}$ and $\mathbf{E}$ are

$$\mathbf{V} = \begin{bmatrix} P_{11} & 0 & 0 & 0 & 0 & 0 \\ 0 & |P_{25}| & 0 & 0 & 0 & 0 \\ 0 & 0 & |P_{36}| & 0 & 0 & 0 \\ 0 & 0 & 0 & -P_{11} & 0 & 0 \\ 0 & 0 & 0 & 0 & -|P_{25}| & 0 \\ 0 & 0 & 0 & 0 & 0 & -|P_{36}| \end{bmatrix},$$

$$\mathbf{E} = \begin{bmatrix} 1 & 0 & 0 & 0 & 0 & 0 \\ 0 & \frac{1}{\sqrt{2}} & 0 & 0 & -\frac{\mathrm{i}}{\sqrt{2}} & 0 \\ 0 & 0 & \frac{1}{\sqrt{2}} & 0 & 0 & -\frac{\mathrm{i}}{\sqrt{2}} \\ 0 & 0 & 0 & 1 & 0 & 0 \\ 0 & \frac{\mathrm{i}}{\sqrt{2}} & 0 & 0 & -\frac{1}{\sqrt{2}} & 0 \\ 0 & 0 & \frac{\mathrm{i}}{\sqrt{2}} & 0 & 0 & -\frac{1}{\sqrt{2}} \end{bmatrix}. \tag{35a, b}$$

Power can thus be transmitted by wave mode 1, wave mode 4, or by the superposition of waves in modes 2 and 5 or in 3 and 6.

(iv) *In region IV*: The power matrix is given by

$$\mathbf{P} = \begin{bmatrix} P_{11} & 0 & 0 & 0 & 0 & 0 \\ 0 & 0 & 0 & 0 & P_{25} & 0 \\ 0 & 0 & P_{33} & 0 & 0 & 0 \\ 0 & 0 & 0 & -P_{11} & 0 & 0 \\ 0 & P_{25}^{*} & 0 & 0 & 0 & 0 \\ 0 & 0 & 0 & 0 & 0 & -P_{33} \end{bmatrix}, \tag{36}$$

where the elements P_{11}, P_{33} and P_{25} are the same as Eqs. (26a), (26c) and (34a), respectively. The element P_{25} is negative-imaginary in this region so that $\mathbf{V}$ and $\mathbf{E}$ are

$$\mathbf{V} = \begin{bmatrix} P_{11} & 0 & 0 & 0 & 0 & 0 \\ 0 & |P_{25}| & 0 & 0 & 0 & 0 \\ 0 & 0 & P_{33} & 0 & 0 & 0 \\ 0 & 0 & 0 & -P_{11} & 0 & 0 \\ 0 & 0 & 0 & 0 & -|P_{25}| & 0 \\ 0 & 0 & 0 & 0 & 0 & -P_{33} \end{bmatrix},$$

$$\mathbf{E} = \begin{bmatrix} 1 & 0 & 0 & 0 & 0 & 0 \\ 0 & \frac{1}{\sqrt{2}} & 0 & 0 & -\frac{\mathrm{i}}{\sqrt{2}} & 0 \\ 0 & 0 & 1 & 0 & 0 & 0 \\ 0 & 0 & 0 & 1 & 0 & 0 \\ 0 & \frac{\mathrm{i}}{\sqrt{2}} & 0 & 0 & -\frac{1}{\sqrt{2}} & 0 \\ 0 & 0 & 0 & 0 & 0 & 1 \end{bmatrix}. \tag{37a, b}$$

Now power is transported independently by wave mode 1, wave mode 3 or a superposition of wave modes 2 and 5.

Fig. 5 shows the magnitudes of the non-zero elements of $\mathbf{P}$ for the curved beam with $\chi^2 = 1/1200$ as a function of a frequency. There are always six energy transport paths at any frequency, but some of these are not shown in the figure (e.g. P_{44}, P_{55} and P_{66} in region I). At high frequencies, the powers associated with the

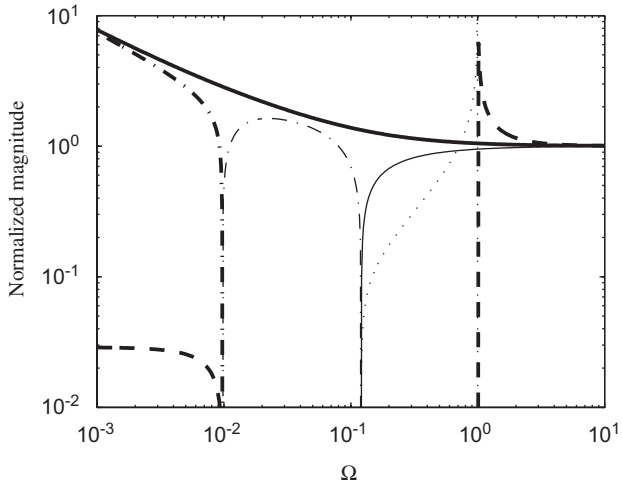

Fig. 5. Non-zero elements of the power matrix for the curved beam with $\chi^2 = 1/1200$: $|P_{11}|$ (——), $|P_{22}|$ (— · —), $|P_{33}|$ (— — —), $|P_{25}|$ (———), $|P_{26}| = |P_{35}|$ (— · — · —), $|P_{36}|$ (·····). In the figure $|P_{33}|$ and $|P_{36}|$ are normalised with respect to ωEAk_L and the others are normalised with respect to $2\omega EIk_B^3$.

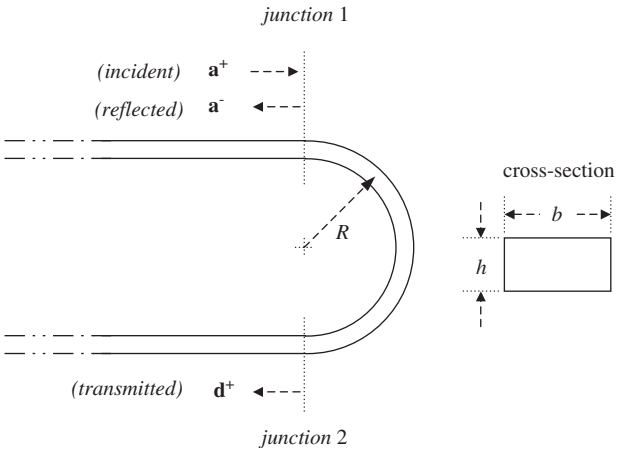

Fig. 6. Reflection and transmission of waves through a curved beam with constant curvature.

waves tend to those of the straight beam: it is seen that the normalised magnitudes of P_{11}, P_{25} and P_{36} tend to unity above the ring frequency $\Omega = 1$.

5. Numerical examples

In this section, two numerical examples are described. The first concerns wave transmission through a curved connector and illustrates how the general matrix formulation can be used to model structures composed of waveguides, some elements of which are curved beams. In the second example, the wave approach is used to calculate natural frequencies of finite structures.

5.1. Wave transmission through a curved beam

The propagation of waves through a curved beam with constant curvature, subtending an angle π and connecting two straight beams as shown in Fig. 6, is considered. The general matrix formulation is applied to

couple the curved beam to the straight regions. The beams all have the same material properties, with rectangular cross-sections of thickness h and width b.

The vector of wave amplitudes incident on the left-hand side of junction 1 is $\mathbf{a}^+$ and the vectors of reflected and transmitted waves are $\mathbf{a}^-$ and $\mathbf{d}^+$, respectively. These vectors are of size 3×1: the first and second elements are the propagating and nearfield waves relating to bending motion of the straight beam, respectively, and the third element is the propagating wave relating to longitudinal motion.

The junctions between the straight and curved regions form discontinuities at which waves are reflected and transmitted. The reflection and transmission matrices can be readily found if the displacement and internal force matrices $\mathbf{\Psi}$ and $\mathbf{\Phi}$ are known for the waveguides (e.g. Ref. [7]). For example, continuity and equilibrium conditions at junction 1 are

$$\mathbf{w}_a = \mathbf{w}_b, \quad \mathbf{f}_a = \mathbf{f}_b, \tag{38a,b}$$

where the subscripts a and b denote the left- and right-hand sides of junction 1, respectively. Incident waves $\mathbf{a}^+$ produce reflected and transmitted waves $\mathbf{a}^-$ and $\mathbf{b}^+$ whose amplitudes are therefore such that

$$\mathbf{\Psi}_a^+\mathbf{a}^+ + \mathbf{\Psi}_a^-\mathbf{a}^- = \mathbf{\Psi}_b^+\mathbf{b}^+, \quad \mathbf{\Phi}_a^+\mathbf{a}^+ + \mathbf{\Phi}_a^-\mathbf{a}^- = \mathbf{\Phi}_b^+\mathbf{b}^+. \tag{39a,b}$$

The matrices $\mathbf{\Psi}_a^\pm$ and $\mathbf{\Phi}_a^\pm$ for a straight beam are given by [7]

$$\mathbf{\Psi}_a^+ = \begin{bmatrix} 1 & 1 & 0 \\ -\mathrm{i}k_B & -k_B & 0 \\ 0 & 0 & 1 \end{bmatrix}, \quad \mathbf{\Phi}_a^+ = \begin{bmatrix} -\mathrm{i}EIk_B^3 & EIk_B^3 & 0 \\ -EIk_B^2 & EIk_B^2 & 0 \\ 0 & 0 & -\mathrm{i}EAk_L \end{bmatrix},$$

$$\mathbf{\Psi}_a^- = \begin{bmatrix} 1 & 1 & 0 \\ \mathrm{i}k_B & k_B & 0 \\ 0 & 0 & 1 \end{bmatrix}, \quad \mathbf{\Phi}_a^- = \begin{bmatrix} \mathrm{i}EIk_B^3 & -EIk_B^3 & 0 \\ -EIk_B^2 & EIk_B^2 & 0 \\ 0 & 0 & \mathrm{i}EAk_L \end{bmatrix}, \tag{40a, b, c, d}$$

while the matrices $\mathbf{\Psi}_b^+$ and $\mathbf{\Phi}_b^+$ for the curved beam are given by Eq. (17a,c). From Eq. (39), the reflection and transmission matrices $\mathbf{R}_1$ and $\mathbf{T}_1$ at junction 1 for waves incident from the left-hand side of junction 1 are given by [7]

$$\mathbf{R}_1 = \left[\mathbf{\Phi}_b^+(\mathbf{\Psi}_b^+)^{-1}\mathbf{\Psi}_a^- - \mathbf{\Phi}_a^-\right]^{-1}\left[-\mathbf{\Phi}_b^+(\mathbf{\Psi}_b^+)^{-1}\mathbf{\Psi}_a^+ + \mathbf{\Phi}_a^+\right],$$
$$\mathbf{T}_1 = \left[\mathbf{\Phi}_a^-(\mathbf{\Psi}_a^-)^{-1}\mathbf{\Psi}_b^+ - \mathbf{\Phi}_b^+\right]^{-1}\left[\mathbf{\Phi}_a^-(\mathbf{\Psi}_a^-)^{-1}\mathbf{\Psi}_a^+ - \mathbf{\Phi}_a^+\right]. \tag{41a, b}$$

The other reflection and transmission matrices $\widehat{\mathbf{R}}_1$, $\widehat{\mathbf{T}}_1$, $\mathbf{R}_2$, $\mathbf{T}_2$, $\widehat{\mathbf{R}}_2$ and $\widehat{\mathbf{T}}_2$ can be obtained in a similar way, the subscripts 1 and 2 referring to junction 1 and 2, while $\widehat{\bullet}$ indicates a matrix for which waves are incident from the right-hand side of the discontinuity. The propagation matrix $\mathbf{F}$ between the junctions is given by Eq. (21). Using the reflection, transmission and propagation matrices, the net reflected and transmitted waves can be expressed as [7]

$$\mathbf{a}^- = \left[\mathbf{R}_1 + \widehat{\mathbf{T}}_1\mathbf{F}\mathbf{R}_2\mathbf{F}[\mathbf{I} - \widehat{\mathbf{R}}_1\mathbf{F}\mathbf{R}_2\mathbf{F}]^{-1}\mathbf{T}_1\right]\mathbf{a}^+, \quad \mathbf{d}^+ = \left[\mathbf{T}_2\mathbf{F}[\mathbf{I} - \widehat{\mathbf{R}}_1\mathbf{F}\mathbf{R}_2\mathbf{F}]^{-1}\mathbf{T}_1\right]\mathbf{a}^+, \tag{42a,b}$$

where $\mathbf{I}$ is the identity matrix.

Consider first the case where a propagating bending wave of amplitude a_1^+ is incident from the left-hand side of junction 1. The incident waves are then $\mathbf{a}^+ = [a_1^+ \quad 0 \quad 0]^{\mathrm{T}}$. The power input to the curved connector is [7]

$$\Pi_i = \omega EIk_B^3|a_1^+|^2. \tag{43}$$

If the amplitudes of the reflected waves are $\mathbf{a}^- = [a_1^- \quad a_2^- \quad a_3^-]^{\mathrm{T}}$, the reflected power is

$$\Pi_r = -\omega EIk_B^3|a_1^-|^2 - \frac{1}{2}\omega EAk_L|a_3^-|^2. \tag{44}$$

Thus the total power reflection coefficient $\varrho = \Pi_r/\Pi_i$ is given by

$$\varrho = \varrho_{BB} + \varrho_{BL}, \tag{45}$$

where

$$\varrho_{BB} = \frac{|a_1^-|^2}{|a_1^+|^2}, \quad \varrho_{BL} = \frac{k_B}{2k_L}\frac{|a_3^-|^2}{|a_1^+|^2}, \tag{46a,b}$$

are the power reflection coefficients for bending-to-bending reflection and bending-to-longitudinal reflection, respectively. Similarly, for transmitted waves $\mathbf{d}^+ = [\,d_1^+ \quad d_2^+ \quad d_3^+\,]^{\mathrm{T}}$, the total power transmission coefficient is given by

$$\tau = \tau_{BB} + \tau_{BL}, \tag{47}$$

where

$$\tau_{BB} = \frac{|d_1^+|^2}{|a_1^+|^2}, \quad \tau_{BL} = \frac{k_B}{2k_L}\frac{|d_3^+|^2}{|a_1^+|^2}. \tag{48}$$

Note that the sum of the coefficients is unity for a conservative system, i.e.,

$$\varrho + \tau = \varrho_{BB} + \varrho_{BL} + \tau_{BB} + \tau_{BL} = 1. \tag{49}$$

Suppose now that the incident waves are $\mathbf{a}^+ = [\,0 \quad 0 \quad a_3^+\,]^{\mathrm{T}}$, i.e., a longitudinal wave of amplitude a_3^+ is incident from the left-hand side of junction 1. The power reflection and transmission coefficients are now

$$\varrho = \varrho_{LB} + \varrho_{LL}, \quad \tau = \tau_{LB} + \tau_{LL}, \tag{50a,b}$$

where

$$\rho_{LB} = \frac{2k_L}{k_B}\frac{|a_1^-|^2}{|a_3^+|^2}, \quad \rho_{LL} = \frac{|a_3^-|^2}{|a_3^+|^2}, \quad \tau_{LB} = \frac{2k_L}{k_B}\frac{|d_1^+|^2}{|a_3^+|^2}, \quad \tau_{LL} = \frac{|d_3^+|^2}{|a_3^+|^2}. \tag{51a,b,c,d}$$

For a conservative system, the sum of these four coefficients is again unity.

Fig. 7 shows the power coefficients for the two cases $\mathbf{a}^+ = [\,a_1^+ \quad 0 \quad 0\,]^{\mathrm{T}}$ and $\mathbf{a}^+ = [\,0 \quad 0 \quad a_3^+\,]^{\mathrm{T}}$. It is seen that $\tau_{BL} = \tau_{BL}$ and $\varrho_{BL} = \varrho_{LB}$ due to reciprocity. Above the ring frequency $\Omega = 1$, τ_{BB} and τ_{LL} are

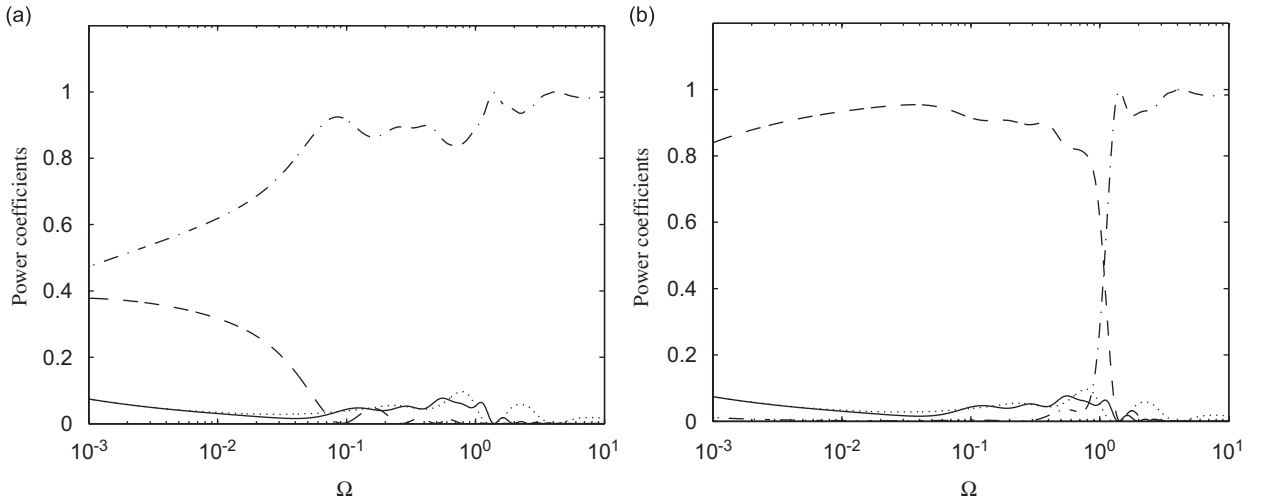

Fig. 7. Power transmission and reflection coefficients for the half-circular beam (a) when a propagating bending wave is incident: τ_{BB} (-·-·-), τ_{BL} (·····), ϱ_{BB} (- - - -), ϱ_{BL} (———) and (b) when a propagating axial wave is incident: τ_{LB} (·····), τ_{LL} (-·-·-), ϱ_{LB} (———), ϱ_{LL} (- - - -).

approximately equal to unity, i.e. the incident waves pass through the junctions and the curved beam freely without scattering or conversion into the other wave mode. Below the ring frequency, the bending wave is substantially transmitted but the longitudinal wave is mainly reflected backwards as a longitudinal wave. For a frequency $\Omega<10^{-2}$, it is seen that $\tau_{BL}\approx\varrho_{BL}$. Furthermore, $\varrho=\varrho_{LB}+\varrho_{LL}=0.5$ (thus $\tau=\tau_{LB}+\tau_{LL}=0.5$) at the ring frequency $\Omega=1$, i.e., half the energy carried by the longitudinal wave is reflected and the other half is transmitted.

5.2. Natural frequencies of finite beams

As a second example, the vibration of a finite, uniform, curved beam is considered. Kang et al. [6] studied the same cases and comparison with their results is made.

Consider a uniform, curved beam subtending an angle θ_L, as shown in Fig. 8, where the radius of curvature of the centreline, R, is constant. The amplitudes of waves at the ends are related by

$$\mathbf{d}^+=\mathbf{F}\mathbf{a}^+,\quad \mathbf{d}^-=\mathbf{R}_L\mathbf{d}^+,\quad \mathbf{a}^-=\mathbf{F}\mathbf{d}^-,\quad \mathbf{a}^+=\mathbf{R}_0\mathbf{a}^-, \tag{52a,b,c,d}$$

where $\mathbf{R}_0$ and $\mathbf{R}_L$ are reflection matrices at the ends ($\theta=0$ and $\theta=\theta_L$), respectively, and $\mathbf{F}$ is the propagation matrix for the curved beam given by Eq. (21). The reflection matrices can be found straightforwardly [7]. For example at $\theta=\theta_L$ the boundary condition is

$$\mathbf{f}=-\mathbf{K}_{\text{ext}}\mathbf{w}, \tag{53}$$

where $\mathbf{K}_{\text{ext}}$ is the dynamic stiffness matrix of the boundary. In terms of the matrices $\mathbf{\Psi}$ and $\mathbf{\Phi}$ it follows that

$$\mathbf{\Phi}^+\mathbf{d}^+ + \mathbf{\Phi}^-\mathbf{d}^- = -\mathbf{K}_{\text{ext}}(\mathbf{\Psi}^+\mathbf{d}^+ + \mathbf{\Psi}^-\mathbf{d}^-) \tag{54}$$

and hence

$$\mathbf{R}_L=-(\mathbf{K}_{\text{ext}}\mathbf{\Psi}^- + \mathbf{\Phi}^-)^{-1}(\mathbf{K}_{\text{ext}}\mathbf{\Psi}^+ + \mathbf{\Phi}^+). \tag{55}$$

Similarly for the end at $\theta=0$

$$\mathbf{R}_0=-(\mathbf{K}_{\text{ext}}\mathbf{\Psi}^+ - \mathbf{\Phi}^+)^{-1}(\mathbf{K}_{\text{ext}}\mathbf{\Psi}^- - \mathbf{\Phi}^-). \tag{56}$$

Rearranging Eq. (52) gives

$$[\mathbf{R}_0\mathbf{F}\mathbf{R}_L\mathbf{F}-\mathbf{I}]\mathbf{a}^+=0. \tag{57}$$

Let $C(\omega)$ be the determinant of the term in the bracket, i.e.,

$$C(\omega)=|\mathbf{R}_0\mathbf{F}\mathbf{R}_L\mathbf{F}-\mathbf{I}|. \tag{58}$$

The frequencies at which $C(\omega)=0$ are the natural frequencies of the beam. These can be found by, for example, root searching methods or the Wittrick–Williams algorithm [9].

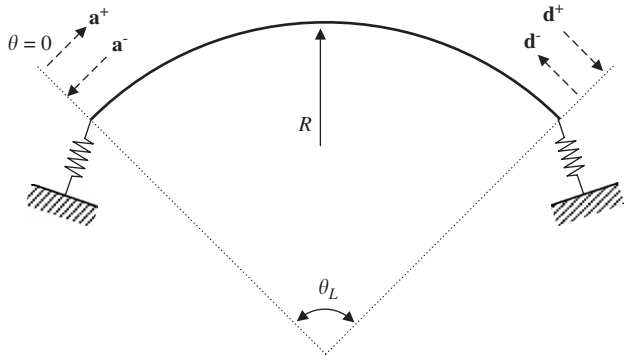

Fig. 8. A finite uniform curved beam with constant curvature.

The non-dimensional frequency

$$\Omega' = \omega R^2 \sqrt{\frac{\rho A}{EI}} \tag{59}$$

is now introduced. Note that $\Omega' = \Omega/\chi$. Fig. 9 shows $C(\Omega')$ for a curved beam with clamped–clamped ends for $\chi^2 = 1/1200$ and $\theta_L = 5^\circ$. The frequencies at which the real and imaginary values of $C(\Omega')$ are both zero are indicated in the plot and are the natural frequencies. Fig. 10 shows the determinant $C(\Omega')$ when the subtended angle $\theta_L = 180^\circ$. Similar figure was seen by Kang et al. [6] (Fig. 7 in their work), although they obtained results based on Love's theory and the present work obtains them based on Flügge's theory.

Table 1 shows the first four non-dimensional natural frequencies Ω' of the uniform curved beam for $\chi^2 = 1/1200$. The results are compared to those obtained by Kang et al. [6]. It seems that the third frequency

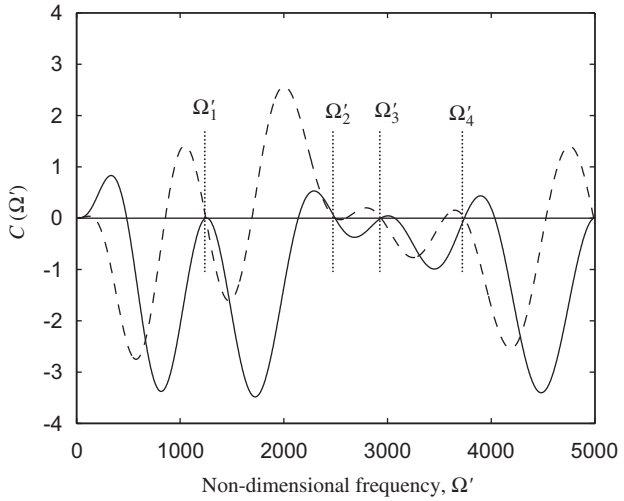

Fig. 9. Determinant $C(\Omega')$ for a uniform circular beam with clamped–clamped ends, $\chi^2 = 1/1200$, $\theta_L = 5^\circ$: Re$[C(\Omega')]$ (solid line), Im$[C(\Omega')]$ (dashed line).

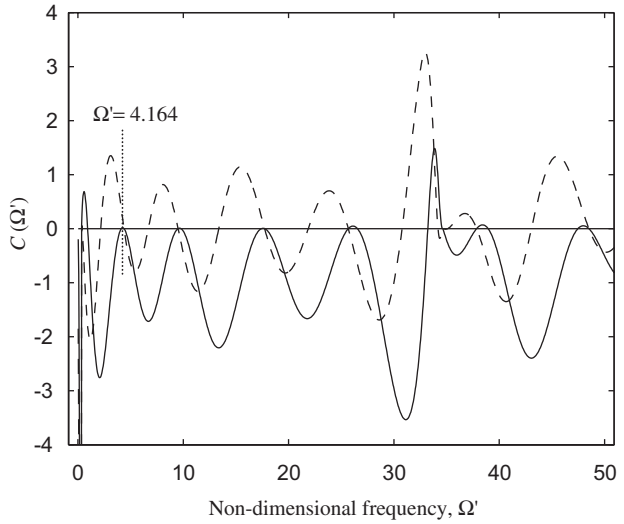

Fig. 10. Determinant $C(\Omega')$ for a uniform circular beam with clamped–clamped ends, $\chi^2 = 1/1200$, $\theta_L = 180^\circ$: Re$[C(\Omega')]$ (solid line), Im$[C(\Omega')]$ (dashed line).

Table 1
Non-dimensional natural frequencies Ω' of a uniform, circular beam for $\chi^2 = 1/1200$

Span angle θ_L (deg)	BC	Mode	Kang et al. [6]	Wave approach
5	Clamped–clamped	1	1247.5675	1247.0700
		2	2489.7481	2493.9590
		3	—	2937.7038
		4	3740.4334	3741.2092
	Free–free	1	1247.1131	1247.4466
		2	2493.9771	2494.2896
		3	2937.7679	2937.2384
		4	3741.4749	3741.4112
180	Clamped–clamped	1	4.3694551	4.3721593
		2	9.4982704	9.5078102
		3	17.704014	17.722215
		4	25.641709	25.668470
	Free–free	1	1.8363460	1.8371547
		2	5.3028579	5.3078041
		3	11.099972	11.111971
		4	18.988464	19.010617

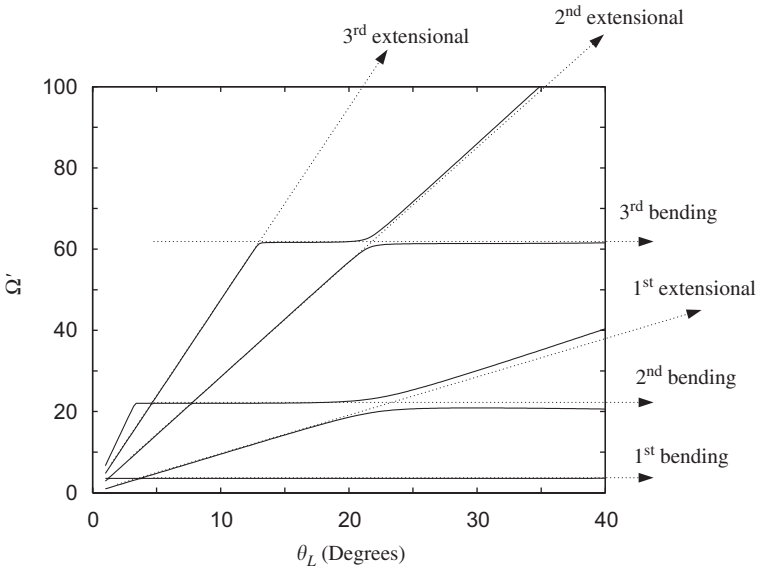

Fig. 11. Natural frequencies of the curved beam (solid lines) and their asymptotic behaviour (dotted lines with arrows) as functions of the subtended angle.

Ω'_3 of the clamped–clamped beam of $\theta_L = 5^\circ$ is missing in the results of Kang et al. Otherwise the differences are primarily due to the fact that the present work is based on Flügge's theory instead of Love's theory.

Fig. 11 shows the first five natural frequencies as functions of the angle θ_L subtended by the beam. In some frequency regions the natural frequencies are more-or-less constant while in other regions they change approximately linearly as θ_L increases. Fig. 11 also shows six further lines. The lines of zero slope are the natural frequencies of the beam undergoing pure bending (or inextensional) motion while the other lines are the frequencies of the beam undergoing pure extensional motion. In various frequency ranges the modes of vibration are dominated by either bending or extensional motion. The results show that the mode sequences changes as θ_L increases, even for the uniform curved beam: for example, when $\theta_L < 4^\circ$ the first mode of the uniform beam is related to the pure extensional motion but when $\theta_L < 4^\circ$ the first mode is related to the pure bending motion.

6. Concluding remarks

This paper concerned in-plane motion of curved beams based on Flügge's theory. Wave propagation was discussed and power considered. Displacement and force matrices were derived—these allow transformations to be made between the physical and wave domains enabling a systematic analysis to be made of waveguide structures with curved components. The energy flow associated with waves in the curved beam was also obtained in a systematic way. It was seen that energy is transported independently by propagating waves or by the interaction of two wave components, for which the wavenumbers are imaginary or a complex conjugate pair. A further transformation to power wave components was found—these components transport power independently.

Numerical results for the power transmission and reflection through a U-shaped structure were obtained using the wave approach based on reflection, transmission and propagation of waves. It was shown that, above the ring frequency, the propagating waves can pass through the curved section with negligible reflection. At the ring frequency, half the energy carried by the longitudinal wave is reflected and the other half is transmitted. A further example was presented to illustrate how the wave approach can be used for the analysis of the vibrations of finite structures.

Appendix A. Cubic equations

The roots of a cubic equation can be found in, for example, Abramowitz and Stegun [10]. Substituting $k^2 = z$ into Eq. (5) gives

$$z^3 + a_2 z^2 + a_1 z + a_0 = 0, \tag{A.1}$$

where

$$a_2 = -(k_L^2 + 2\kappa^2), \quad a_1 = \kappa^4 - k_B^4 + 2\kappa^2 k_L^2, \quad a_0 = -(\kappa^4 k_L^2 + \kappa^2 k_B^4 - k_L^2 k_B^4). \tag{A.2a,b,c}$$

Now let

$$r = (9a_2a_1 - 27a_0 - 2a_2^3)/54, \quad q = (3a_1 - a_2^2)/9 \tag{A.3a,b}$$

and

$$s_1 = \left(r + \sqrt{q^3 + r^2}\right)^{1/3}, \quad s_2 = \left(r - \sqrt{q^3 + r^2}\right)^{1/3}. \tag{A.4a,b}$$

The three roots z_1, z_2 and z_3 of the cubic Eq. (A.1) are then

$$\begin{aligned} z_1 &= -\frac{1}{3}a_2 + (s_1 + s_2), \\ z_2 &= -\frac{1}{3}a_2 - \frac{1}{2}(s_1 + s_2) + \mathrm{i}\frac{\sqrt{3}}{2}(s_1 - s_2), \\ z_3 &= -\frac{1}{3}a_2 - \frac{1}{2}(s_1 + s_2) - \mathrm{i}\frac{\sqrt{3}}{2}(s_1 - s_2). \end{aligned} \tag{A.5a, b, c}$$

Note that the three roots z_1, z_2 and z_3 satisfy

$$z_1 + z_2 + z_3 = -a_2, \quad z_1z_2 + z_2z_3 + z_3z_1 = a_1, \quad z_1z_2z_3 = -a_0. \tag{A.6a,b,c}$$

These results are used for the discussion in Section 4 of the power associated with the wave components. When damping is neglected, the quantity $q^3 + r^2$ in Eq. (A.4) is real since a_2, a_1 and a_0 are all real. If $q^3 + r^2 > 0$, one root is real and two are complex conjugates; if $q^3 + r^2 = 0$, three roots are real and at least two are equal; and if $q^3 + r^2 < 0$, three roots are real and unequal. When damping exists, the three roots become complex.

The six wavenumbers are given by $\pm\sqrt{z_i}$, where $i = 1, 2, 3$, as shown in Fig. 2. The bifurcation points in Fig. 2 are at the frequencies where $q^3 + r^2 = 0$. Note that there is an ambiguity in defining each frequency relationship for z_1, z_2 and z_3 [11]. This ambiguity arises in calculating the square and cube roots in Eq. (A.4).

It can be partly removed by defining the cube root of a real quantity to be real. In any event, the roots are associated with positive or negative going waves by the criterion given in Eq. (9).

Appendix B. Energy flow in curved beams

The values of P_{mn} are obtained for all possible pairs of the six wave components. In Section 3, $\boldsymbol{\psi}_i$ and $\boldsymbol{\phi}_i$ for $i = 3, 6$ do not have the same form as $\boldsymbol{\psi}_i$ and $\boldsymbol{\phi}_i$ for $i = 1, 2, 4, 5$. However using these definitions would make the following discussion unnecessarily long. Thus, for the time being, $\boldsymbol{\psi}_i$ and $\boldsymbol{\phi}_i$ for $i = 3, 6$ are assumed to be of the same form as that given in Eq. (18). This assumption will not affect the qualitative investigation of P_{mn} since the difference only comes from dividing by the displacement ratio α_3 or α_6. Under this assumption, Eq. (24) can be written as

$$P_{mn} = \frac{\omega}{2}\left\{EI(k_n + k_m^*)\left(k_n^2 + (k_m^*)^2 - 2\kappa^2\right) + EA(k_n + k_m^*)\alpha_n\alpha_m^* - \mathrm{i}EA\kappa(\alpha_n - \alpha_m^*)\right\}. \tag{B.1}$$

Substituting Eq. (11) for the displacement ratio into Eq. (B.1) gives

$$P_{mn} = \frac{\omega EI(k_n + k_m^*)}{2}\left\{k_n^2 + (k_m^*)^2 - 2\kappa^2 + \frac{k_B^4\kappa^2}{(k_L^2 - k_n^2)(k_L^2 - (k_m^*)^2)}\right\}. \tag{B.2}$$

Note again that Eq. (B.2) is only true for P_{mn} for $m = 1, 2, 4, 5$ and $n = 1, 2, 4, 5$, respectively. When the components of the third mode are concerned (i.e. m or n is 3 or 6, respectively), it should be divided again by α_3, α_6, or their self- or cross-product as required.

B.1. Energy flow due to a single wave component

The diagonal elements of the matrix $\mathbf{P}$ are related to the energy carried by a single wave component. When $n = m$, Eq. (B.2) becomes

$$P_{mm} = \frac{\omega EI(k_m + k_m^*)}{2}\left\{k_m^2 + (k_m^*)^2 - 2\kappa^2 + \frac{k_B^4\kappa^2}{(k_L^2 - k_m^2)(k_L^2 - (k_m^*)^2)}\right\}. \tag{B.3}$$

There are three cases for the wavenumber k_m.

(i) *Purely imaginary wavenumber*: The first parenthesised term in Eq. (B.3) indicates that, if k_m is purely imaginary (i.e., the wave mode is evanescent), the element will be zero. Thus $P_{22} = P_{44} = 0$ in regions III and IV.

(ii) *Purely real wavenumber*: If k_m is purely real (i.e. $k_m^* = k_m$), Eq. (B.3) reduces to

$$P_{mm} = \omega EIk_m\left\{2(k_m^2 - \kappa^2) + \frac{k_B^4\kappa^2}{(k_L^2 - k_m^2)^2}\right\}. \tag{B.4}$$

Eq. (B.4) holds for wave components $m = 1, 2, 4, 5$. For the third mode (i.e. $m = 3, 6$), it becomes

$$P_{mm} = \frac{\omega EIk_m}{|\alpha_m|^2}\left\{2(k_m^2 - \kappa^2) + \frac{k_B^4\kappa^2}{(k_L^2 - k_m^2)^2}\right\} = \omega EA\frac{k_L^2}{k_m}\left\{1 + \frac{2(k_m^2 - \kappa^2)(k_L^2 - k_m^2)^2}{k_B^4\kappa^2}\right\}. \tag{B.5}$$

When κ is small so that the terms involving κ can be neglected with respect to k_m and k_m asymptotes to the bending or longitudinal wavenumbers of the straight beam, Eqs. (B.4) and (B.5) asymptote to those for the straight beam as expected.

(iii) *Complex wavenumber*: Now assume k_m is not purely real or purely imaginary. The wavenumber k_m and its complex conjugate k_m^* satisfy the characteristic equation

$$k_m^6 + a_2k_m^4 + a_1k_m^2 + a_0 = 0, \quad (k_m^*)^6 + a_2(k_m^*)^4 + a_1(k_m^*)^2 + a_0 = 0, \tag{B.6a,b}$$

where a_2, a_1 and a_0 are the coefficients given by Eq. (A.2). Subtracting Eq. (B.6a) from Eq. (B.6b) gives

$$\{k_m^2 - (k_m^*)^2\}\{k_m^4 + k_m^2(k_m^*)^2 + (k_m^*)^4 + a_2(k_m^2 + (k_m^*)^2) + a_1\} = 0. \tag{B.7}$$

Since the first bracketed term in Eq. (B.7) will not be zero if k_m is not purely real or purely imaginary, it follows that

$$k_m^4 + k_m^2(k_m^*)^2 + (k_m^*)^4 + a_2(k_m^2 + (k_m^*)^2) + a_1 = 0. \tag{B.8}$$

Using Eq. (B.8) it can be shown that the bracketed term in Eq. (B.3) is zero for complex k_m.

According to the discussion above, a single wave component can transport energy only when the wavenumber is purely real, as expected.

B.2. Energy flow due to two opposite-going waves of one mode

The non-diagonal elements of **P** are related to energy carried by the interaction between two different wave components. First consider the case that a positive-going wave component of one mode interacts with the negative-going component of the same mode, or vice versa. Six elements of the power matrix are relevant to this case, i.e. P_{14}, P_{25}, P_{36}, P_{41}, P_{52} and P_{63}. The power matrix is Hermitian so that the first three elements are complex conjugates of the latter three elements. Since $k_n = -k_m$ in this case, Eq. (B.2) becomes

$$P_{mn} = \frac{\omega EI(-k_m + k_m^*)}{2}\left\{k_m^2 + (k_m^*)^2 - 2\kappa^2 + \frac{k_B^4\kappa^2}{(k_L^2 - k_m^2)(k_L^2 - (k_m^*)^2)}\right\}. \tag{B.9}$$

Eq. (B.9) is the same as Eq. (B.3) except for the first parenthesised term. Thus the interaction between two opposite-going wave components of one mode can transport energy only when the wavenumber is purely imaginary: if k_m is real, the first parenthesised term is zero, and if k_m is complex, the bracketed term is zero. Therefore $P_{14} = P_{41} = 0$ for all frequencies, P_{25} and P_{52} are non-zero in regions III and IV, and P_{36} and P_{63} are non-zero in region III. The non-zero element P_{25} is

$$P_{25} = -\omega EIk_2\left\{2(k_2^2 - \kappa^2) + \frac{k_B^4\kappa^2}{(k_L^2 - k_2^2)^2}\right\} \tag{B.10}$$

and the non-zero element P_{36}, after allowing for the normalisation with respect to α_3 and α_6, is

$$P_{36} = -\omega EA\frac{k_L^2}{k_3}\left\{1 + \frac{2(k_3^2 - \kappa^2)(k_L^2 - k_3^2)^2}{k_B^4\kappa^2}\right\}. \tag{B.11}$$

Note again that the counterpart elements P_{52} and P_{63} are the complex conjugates of P_{25} and P_{36}, respectively.

B.3. Energy flow due to two different wave modes

Now consider the case that a wave component of one mode interacts with a component of another mode. The elements P_{12}, P_{13}, P_{15}, P_{16}, etc., of the power matrix are relevant to this case. Since k_m and k_n in Eq. (B.2) are different wavenumbers, it follows from Eq. (A.6) that

$$(k_L^2 - k_m^2)(k_L^2 - k_n^2)(k_m^2 + k_n^2 - 2\kappa^2) + k_B^4\kappa^2 = 0. \tag{B.12}$$

Substituting $k_B^4\kappa^2$ from Eq. (B.12) into Eq. (B.2) yields

$$P_{mn} = \frac{\omega EI(k_n + k_m^*)\{k_m^2 - (k_m^*)^2\}\{k_m^2 + (k_m^*)^2 + k_n^2 - k_L^2 - 2\kappa^2\}}{2(k_L^2 - (k_m^*)^2)}. \tag{B.13}$$

Using the wavenumber k_o for the third mode, which is related through Eq. (A.6a) to k_m and k_n, Eq. (B.13) reduces to

$$P_{mn} = \frac{\omega EI(k_n + k_m^*)\{k_m^2 - (k_m^*)^2\}\{(k_m^*)^2 - k_o^2\}}{2(k_L^2 - (k_m^*)^2)}. \tag{B.14}$$

(i) The first bracketed term in the numerator of Eq. (B.14) indicates that the interaction of the two components cannot transport energy if the wavenumber for one of the two interacting waves is purely real or purely imaginary. Thus $P_{12} = P_{13} = P_{15} = P_{16} = 0$, $P_{42} = P_{43} = 0$, and $P_{54} = P_{64} = 0$ for all frequencies.

(ii) Only P_{23}, P_{26} and P_{35} (and their counterparts) in the matrix **P** have not been considered yet. These elements are related to energy transported by interaction between a wave component of the second mode and a wave component of the third mode. Since at least one wavenumber for the two modes is purely real or purely imaginary in the whole frequency range except region II, P_{23}, P_{26} and P_{35} are zero over most of the frequency range. The first parenthesised term in the numerator of Eq. (B.14) indicates that, even in region II, P_{23} is zero since $k_3 = -k_2^*$. As a result, P_{26} and P_{35} are non-zero in region II. Since $k_6 = k_2^*$ in region II, after allowing for the normalisation with respect to α_6, P_{26} in this region is given by

$$P_{26} = -\frac{i\omega EI}{\kappa}(k_2^2 - (k_2^*)^2)((k_2^*)^2 - k_1^2). \tag{B.15}$$

In region II, P_{35} is also non-zero and $P_{35} = P_{26}^*$.

References

[1] J.P. Charpie, C.B. Burroughs, An analytical model for the free in-plane vibration of beams of variable curvature and depth, *Journal of the Acoustical Society of America* 94 (1993) 866–879.
[2] P. Chidamparam, A.W. Leissa, Vibrations of planar curved beams, rings and arches, *Applied Mechanics Reviews* 46 (1993) 467–483.
[3] N.M. Auciello, M.A. De Rossa, Free vibrations of circular arches: a review, *Journal of Sound and Vibration* 176 (1994) 433–458.
[4] C.M. Wu, B. Lundberg, Reflection and transmission of the energy of harmonic elastic waves in a bent bar, *Journal of Sound and Vibration* 190 (1996) 645–659.
[5] S.J. Walsh, R.G. White, Vibrational power transmission in curved beams, *Journal of Sound and Vibration* 233 (2000) 455–488.
[6] B. Kang, C.H. Riedel, C.A. Tan, Free vibration analysis of planar curved beams by wave propagation, *Journal of Sound and Vibration* 260 (2003) 19–44.
[7] S.-K. Lee, Wave Reflection, Transmission and Propagation in Structural Waveguides, PhD Thesis, Southampton University, 2006.
[8] R.S. Langley, A transfer matrix analysis of the energetics of structural wave motion and harmonic vibration, *Proceedings of the Royal Society of London A* 452 (1996) 1631–1648.
[9] W.H. Wittrick, F.W. Williams, A general algorithm for computing natural frequencies of elastic structures, *Quarterly Journal of Mechanics and Applied Mathematics* 24 (1971) 263–284.
[10] M. Abramowitz, I.A. Stegun, *Handbook of Mathematical Functions with Formulas, Graphs, and Mathematical Tables*, Dover Publications, New York, 1965.
[11] J.F. Doyle, *Wave Propagation in Structures: Spectral Analysis using Fast Discrete Fourier Transforms*, Springer, New York, 1997.